Channel Capacity and Achievable Rates of Peak Power Limited AWGNC, and their Applications to Adaptive Modulation and Coding

Shiro Ikeda
The Institute of Statistical Mathematics
Graduate Univ. for Advanced Studies
Tokyo, 190-8562, Japan

Kazunori Hayashi
Kyoto University
Department of Systems Science
Kyoto, 606-8501, Japan

Toshiyuki Tanaka
Kyoto University
Department of Systems Science
Kyoto, 606-8501, Japan

***Abstract*—The channel conditions vary over time in wireless communications. In order to transmit information efficiently, digital wireless communication systems choose the modulation scheme and coding adaptively. This framework is called the adaptive modulation and coding (AMC). The key problem of the framework is how to design the switching strategy. In this paper, we discuss the practical strategy for AMC by comparing the channel capacity, achievable rates with common modulation schemes, and the actual rates with AMC. The channel capacity is defined for a combination of the noisy channel and the constraint on the information source. The noisy channel we assume in this paper is the discrete-time complex-valued additive white Gaussian noise channel (AWGNC). For the constraint, we focus on the peak power instead of the average power since a practical communication transmitter often suffers from the peak power. We compare the capacity and achievable rates with practical modulation schemes. Furthermore, we simulate AMC and evaluate the actual rates numerically.**

I. Introduction

In digital wireless communication systems, it is important to use appropriate modulation scheme and coding in order to transmit information efficiently. The conditions of a wireless communication channel change over time and a single set of modulation scheme and coding may not be efficient for all the conditions. In order to realize an efficient transmission, adaptive modulation and coding (AMC) [1] is utilized, where modulation scheme and coding are switched adaptively according to the channel conditions. In this paper, we discuss the switching scheme of AMC.

We first show the channel capacity. The channel capacity is defined as the supremum of the mutual information between input and output [2], where the supremum is taken under a constraint on the input. In the following, the channel is assumed to be a complex-valued additive white Gaussian noise channel (AWGNC). For a band-limited channel, a well-known result is the Shannon-Hartley theorem, that is, the capacity $W\log(1+\mathsf{SNR})$ (SNR: signal-to-noise ratio) for an AWGNC with a bandwidth of W under the average power constraint on the input. This is an important formula, found in almost all textbooks on communication theory. However, a real-world communication system suffers from limitations other than the average power. From an engineering viewpoint, the peak power constraint is important, because the power amplifier of a communication system has an absolute peak power (amplitude) limitation. We also note that power efficiency of an amplifier largely depends on the peak value of the continuous-time input signal [3]. Under the peak power constraint, the quantity $W\log(1+\mathsf{SNR})$ is no longer the capacity. Theoretically, the channel capacity and the capacity achieving distribution (CAD) for an AWGNC under the peak power constraint have been studied [4], [5]. The CAD is proved to be discrete and the channel capacity is computed numerically.

Although the CAD is discrete, they may not be identical to the modulation scheme of digital communication systems. Thus, the channel capacity is compared to the achievable rates with typical modulation schemes, such as phase shift keying (PSK), quadrature amplitude modulation (QAM) and amplitude and phase shift keying (APSK). These modulation schemes are typically used in AMC. Therefore, this numerical simulation shows the practical bound for AMC. It is demonstrated that if a modulation scheme is chosen properly, the discrepancy between the capacity and the best achievable rate is not large.

The achievable rates provide a useful guideline to choose the best modulation scheme. After choosing the modulation scheme, we need to choose the coding. In order to see how close we can reach by choosing the coding, some numerical results are shown. They show the rate of AMC can be fairly close to the achievable rates if the coding is chosen properly.

From these comparisons, we reveal the fact that the best achievable rates are surprisingly close to the capacity and the rates with AMC can be close to the achievable rates. Our results imply that a well-designed AMC can achieve a rate which is very close to the capacity.

II. Capacity

The channel capacity is the upper bound of the transmission rate. In this section, the capacity and the CADs of this communication channel are shown under reasonable constraints on the inputs are reviewed.

A. AWGNC and Peak Power Constraints

In this paper, we consider a discrete-time complex-valued AWGNC, which is memoryless and having an isotropic independent Gaussian noise,

$$\begin{pmatrix} Y_I \\ Y_Q \end{pmatrix} = \begin{pmatrix} X_I \\ X_Q \end{pmatrix} + \frac{\sigma}{\sqrt{2}} \begin{pmatrix} N_I \\ N_Q \end{pmatrix}, N_I, N_Q \sim \mathcal{N}(0,1), \quad (1)$$

where X_I and X_Q denote in(I)- and quadrature(Q)-phase input components, respectively.

In order to compute the capacity, a constraint on the input must be defined. Although the average power constraint is commonly assumed, we take the peak power constraint. There are mainly two reasons. Firstly, for the single-carrier transmitter, the average power consumption of the amplifier is dominated by back-off [3], and it is therefore more reasonable to compare different modulation schemes, in other words signal constellations, by aligning their amplitudes in terms not of their average power but of their peak power. Secondly, the capacity $\log(1 + \mathsf{SNR})$ is achieved only by a Gaussian input distribution whose support is unbounded. This cannot be realized under peak power constraint.

There are two distinctive natural forms of peak power constraint for wireless digital communications systems, according to different implementations of the transmitter front-end. Let us assume that amplifiers of a system have equal peak power bounds. If each of X_I and X_Q has an amplifier separately, a natural form of peak power constraint is the component-wise constraint $X_I^2, X_Q^2 \leq E_{\max}/2$. We call this the *box constraint*. Another implementation is that the sum of the components is amplified at once. The peak power constraint in this case is formulated as $X_I^2 + X_Q^2 \leq E_{\max}$, which we call the *circular constraint*.

Let $\mathsf{pSNR} = E_{\max}/\sigma^2$ denote the ratio of peak input power to the noise variance, which we call peak SNR. Under the peak power constraint, the capacity of the AWGNC defined in eq. (1) must be smaller than $\log(1 + \mathsf{pSNR})$ for two reasons: i) $\mathsf{pSNR} \geq \mathsf{SNR}$ holds and ii) the input distribution cannot be Gaussian. It is known that the CAD for the AWGNC under peak power constraint becomes discrete. This phenomenon was first shown for a scalar AWGNC [4], and has been extended for many channels with different constraints [5]–[8]. Using these results, we numerically evaluate the capacity under each of the box and circular constraints in the following subsections.

B. Box Constraint

Under the box constraint, the I- and Q-components of the channel defined in eq.(1) suffer from independent Gaussian channel noises as well as independent peak power constraints. Accordingly, the channel is decomposed into two independent real-valued AWGNCs under the respective peak power constraints $X_I^2 \leq E_{\max}/2$ and $X_Q^2 \leq E_{\max}/2$. The capacity of the complex-valued AWGNC is thus attained by the direct product of CADs of the two real-valued AWGNCs under peak power constraint.

The capacity of a real-valued AWGNC under the peak power constraint has been studied by Smith [4]. He has proved that the capacity is achieved by a discrete input distribution with a finite number of probability mass points. Although no analytical solution is known for the capacity itself, nor the CAD, one can evaluate them numerically via the method described in [4] with Gauss-Hermite integration. Figure 1a shows the positions of the probability mass points of the CAD versus pSNR. The points are symmetrically positioned around 0 and two points are always located at the boundaries $\pm\sqrt{E_{\max}/2}$. The number of the probability mass points of the CAD is 2 for low enough pSNRs and increases as pSNR becomes larger. It is in contrast with the case under average power constraint, where the CAD is Gaussian and remains essentially the same irrespective of noise level.

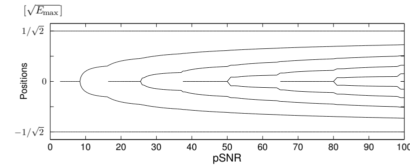

(a) Locations of mass points of CADs for a real-valued scalar AWGNC.

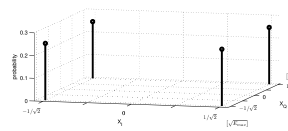

(b) CAD for $\mathsf{pSNR} = 1$.

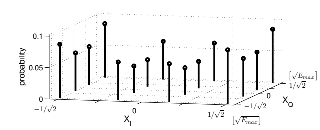

(c) CAD for $\mathsf{pSNR} = 16$.

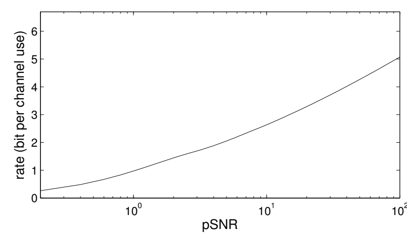

(d) Capacity under box constraint.

Fig. 1. CADs and capacity for AWGNC under box constraint.

The CAD for the complex-valued AWGNC under the box constraint is obtained by taking the direct product of the above CADs. One immediate consequence from Fig. 1a is that QPSK is the optimal modulation scheme for small enough pSNR (Fig. 1b). For a larger pSNR, the CAD becomes similar to nQAM, where $n = m^2$ ($m \geq 2; m \in \mathbb{N}$) (Fig. 1c). Note that probability masses of the points of a CAD are generally not equal for $m > 2$. The capacity is computed numerically and plotted in Fig. 1d.

C. Circular Constraint

The capacity and the joint distribution of X_I and X_Q which achieves the capacity under the circular constraint have been studied in [5]. The result is best described with the polar coordinate. Reparameterizing X_I and X_Q with the radius r and the phase ϕ, the CAD is uniform for ϕ and discrete with a finite number of probability mass points for r. Consequently, the CAD consists of concentric circles centered at the origin. The number of the circles and their radii, as well as their probability weights vary with pSNR. Analytical solution is not available, however, one can compute the capacity and the CAD numerically via the method described in [5] with Gauss-Laguerre integration.

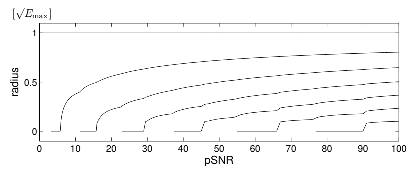

(a) Locations of mass points of CADs in radial coordinate under circular constraint.

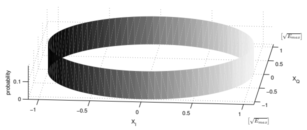

(b) CAD for $\mathsf{pSNR} = 1$.

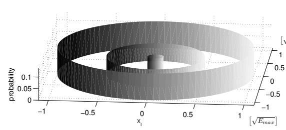

(c) CAD for $\mathsf{pSNR} = 16$.

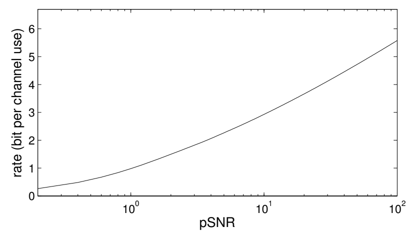

(d) Capacity under circle constraint.

Fig. 2. CADs and capacity for AWGNC under circular constraint.

Figure 2 shows the numerically computed CADs under the circular constraint $X_I^2 + X_Q^2 \leq E_{\max}$. Figure 2a shows radial positions of probability masses of the CADs. The number of the radial points is 1 for small enough pSNRs, while it increases as pSNR becomes larger. One of the points is always located at the boundary $r = \sqrt{E_{\max}}$. Accordingly, the CAD is a single circle for a small pSNR (Fig. 2b) and multiple concentric circles for a larger pSNR (Fig. 2c). The capacity is computed numerically and plotted in Fig. 2d. It becomes larger than that in Fig. 1d because the admissible region of $X_I^2 + X_Q^2 \leq E_{\max}$ is bigger than $X_I^2, X_Q^2 \leq E_{\max}/2$.

III. Achievable Rates with Widely Used Constellations

A list of modulation schemes are prepared in AMC, and one of them is chosen from the list. Thus, the maximum of the achievable rates with these modulation schemes will provide the upper bound of the AMC. The achievable rates with typical modulation schemes are compared to the capacity.

A. Box Constraint

Figure 3 shows the achievable rates with nQAMs and the capacity under the box constraint. One can observe that each of the achievable rates comes very close to the capacity around intermediate pSNR values, and that the pSNR range in which the achievable rate with nQAM comes close to the capacity shifts rightwards as n increases. This observation is ascribed to the fact that the nQAMs are similar in their shapes to the CADs under the box constraint in the respective pSNR ranges.

The above results also indicate that appropriate switching between nQAMs with different n will achieve rates that are close to the capacity under the box constraint. For example, among QPSK, 16QAM, and 64QAM, the best is QPSK for pSNR smaller than 6, 16QAM for pSNR values between 6 and 35, and 64QAM for larger pSNR. From Fig. 3, the degradation of the achievable rate with the above discrete adaptive modulation from the capacity in terms of pSNR for the rates 1, 2, and 3 are 0.0, 1.0, and 0.012 dB, respectively.

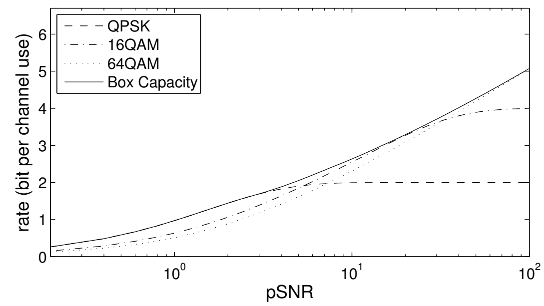

Fig. 3. Achievable rates with QPSK, 16QAM, and 64QAM compared with capacity under box constraint.

B. Circular Constraint

The achievable rates with different modulation schemes are shown along with the capacity under the circular constraint in Fig. 4. The achievable rate with QPSK is very close to the capacity for small pSNRs. One also observes that 16PSK, although not popular in current communications systems, has the achievable rate closer to the capacity up to a moderate value of pSNR. Increasing the number n of signal points in nPSK makes the achievable rate closer to the capacity up to a yet larger pSNR value, but the rate becomes falling off from the capacity beyond that pSNR value (Fig. 4). Figure 2a explains the reason. As the number n of nPSK increases, the input distribution approaches a single circle, while the number of the circles increases for the CAD.

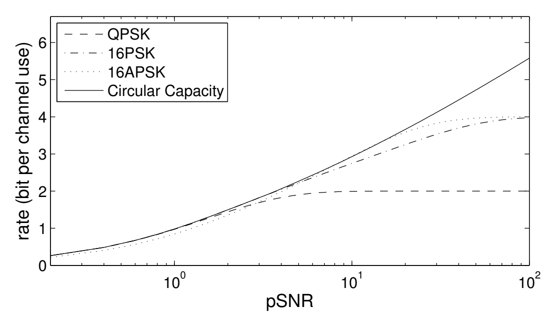

Fig. 4. Achievable rates with QPSK, 16PSK, and 16APSK compared with capacity under circular constraint.

As is the case under the box constraint, one can expect that a higher rate should be achievable by designing the input distribution so as to make it similar to the CAD under the circular constraint. The shapes of CADs under the circular constraint imply that amplitude and phase shift keying (APSK)-type modulations work better than PSKs for a larger pSNR. Use of APSK modulations under the circular constraint has been studied in [9]. As an example, we consider in this paper

16APSK, where the 16 points are defined as follows,

$$(X_I, X_Q) = \sqrt{E_{\max}}\Big(\cos\frac{\pi k}{6}, \sin\frac{\pi k}{6}\Big),\ \ k = 0, \dots, 11,$$
$$\frac{\sqrt{2E_{\max}}}{3}\Big(\cos\frac{(2l+1)\pi}{4}, \sin\frac{(2l+1)\pi}{4}\Big),\ \ l = 0, \dots, 3,$$

which is intended to mimic the CAD with pSNR $\sim$ 10 consisting of two circular components. The achievable rate with 16APSK is compared with those of PSKs and the capacity under the circular constraint in Fig. 4. As we have expected, the achievable rate with 16APSK is worse than those of PSKs for a pSNR less than around 5 but is very close to the capacity under the circular constraint for a larger pSNR up to around 20. Note that pSNR of 5 corresponds to the point where the number of the circles of the CAD increases from 1 to 2 in Fig. 2a. Thus we expect the APSK with more amplitude shifts would have good achievable rates for a larger pSNR and that curves like those shown in Fig. 4 would indicate the corresponding pSNR to switch between them.

IV. Adaptive Modulations and Codes

In this section, we evaluate the rates with practical schemes, namely, the combined use of the discrete modulations and low-density parity check codes (LDPCC), under peak power constraint. The rates are computed numerically, and compared with the achievable rates with corresponding modulation schemes shown in section III. The LDPCCs used in the simulation are the codes employed in the DVB-S2 standard [10], where the codeword length is 64800 and the coding rates are $1/4$, $1/3$, $2/5$, $1/2$, $3/5$, $2/3$, $3/4$, $4/5$, $5/6$, $8/9$, and $9/10$. Gray coded bit mapping is used for QPSK, 16QAM, and 16PSK, while the mapping defined in the DVB-S2 standard is used for 16APSK.

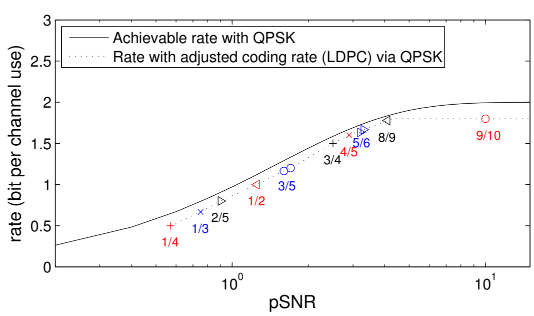

Fig. 5. Rates with adjusted coding rate LDPCC via QPSK versus pSNR.

Figure 5 shows the numerical results of the rates with adjusted coding rate LDPCC via QPSK versus pSNR. The rate of the practical scheme is defined as

$$\text{rate} = \frac{S_{\text{blck}}}{T_{\text{blck}}} r \log_2 n,$$

where r denotes coding rate, T_{blck} the number of LDPCC blocks sent from the transmitter, S_{blck} the number of LDPCC blocks received without errors, and n is the number of points of the constellation. The achievable rate with QPSK is also shown as a reference. From the figure, we see that, by appropriate choice of the coding rate, the practical modulation and coding, i.e., QPSK and LDPCC, achieve the rate close to the achievable rate with QPSK, which is very close to the achievable rate.

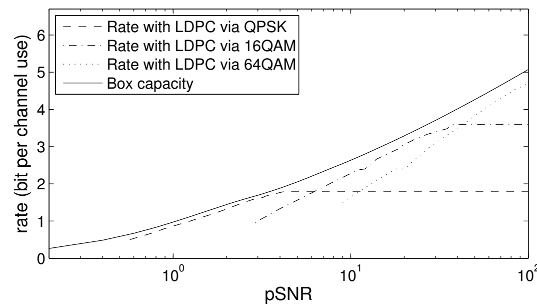

Fig. 6. Achievable rates with QPSK, 16QAM, and 64QAM compared with capacity under box constraint.

The rates with LDPCC via QPSK, 16QAM, and 64QAM versus pSNR are shown in Fig. 6, where the capacity under the box constraint is also plotted. The qualitative characteristics is very similar to Fig. 3, and as expected in section III-A, it is possible to achieve rates close to the capacity by switching modulation schemes and coding rates appropriately. Note that the switching thresholds of pSNR agree well with those expected from Fig. 3.

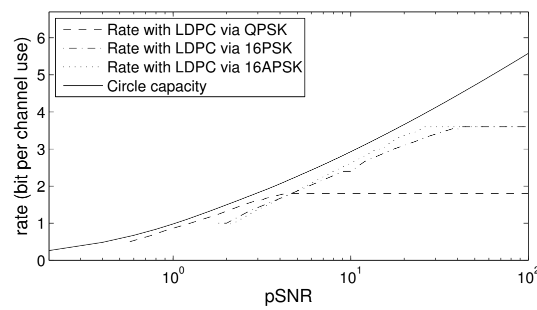

Fig. 7. Achievable rates with QPSK, 16PSK, and 16APSK compared with capacity under circular constraint.

Finally, the rates with LDPCC via QPSK, 16PSK, and 16APSK versus pSNR are shown in Fig. 7 with the capacity under circular constraint. The results agree with those in Fig. 4 again, which demonstrates the validity of the discussion in section III-B even for the case with practical discrete adaptive modulation and coding.

These results indicate a possible strategy for AMC. When a pSNR, which reflects the channel condition is given, the modulation can be chosen according to the achievable rate of each modulation scheme and then, the coding rate is chosen in order to achieve the rate close to the capacity. This is different from the strategy used in general, where modulation and coding rate are optimized jointly for a given channel quality.

V. Conclusion

For digital communications systems, choosing an appropriate modulation scheme is a key issue. We can find some plots for comparison in literature (see [11, Sec. 11.3] for example), where the achievable rates for the AWGNC with practical modulation scheme, such as PSKs and QAMs, are shown versus SNR. Such a plot usually includes a curve indicating Shannon's capacity $\log(1+\mathsf{SNR})$, which is the capacity for the AWGNC under the average input power constraint. A natural observation from such a plot is that the achievable rates with nQAM ($n \geq 16$) input constellations are almost always closer to the capacity than those with PSKs. This implies that, if we assume a system with adaptive modulation which can use QPSK, 16PSK, and 16QAM, then such a system should always choose 16QAM, neglecting the complexity in implementation.

The above comparison is well-known, but not appropriate in practice. In this paper, we have compared the capacity, the achievable rates, and the rates of AMC under peak power (Box and Circular) constraints on input. The importance of the peak power constraint has been realized, but it has mostly been considered only indirectly via the peak-to-average power ratio (PAR) [12]. Indeed, typical conventional arguments define the capacity under the average power constraint, and discuss the peak power (or the power efficiency) only via PAR. On the other hand, the direct approach in this paper allows us to evaluate quantitatively how close the achievable rates to the theoretical limit posed by the capacity under a practical constraint on input. The proposed approach provides a fresh look at the problem of comparing performance between different modulation schemes. A major weakness with our approach would be that one can no longer expect a simple closed-form expression for the capacity, such as $W\log(1+\mathsf{SNR})$, so that evaluation of the capacity itself might be elaborative and computationally intensive. We nevertheless believe, despite this weakness, the significance of our approach in view of better understanding of the room for improvement toward the theoretical limit under practical constraints.

In order to demonstrate the significance of our approach, we have studied, as an example, the capacity of a complex-valued AWGNC under peak power constraint on discrete-time signal and compare it with the achievable rates with practical modulation schemes and rates with AMC. We have observed that the achievable rates with nQAM are very close to the capacity under the box constraint for some range of pSNR, and that the range shifts to larger pSNR as the modulation level n of nQAM increases. We have also observed that the achievable rates with nPSK are very close to the capacity under the circular constraint for small pSNR. Our results have also suggested that APSK-type modulation is expected to have an achievable rate close to the capacity under the circular constraint for larger pSNR. The achievable rate with 16APSK has been computed to support this expectation. These results, as well as the results in [9] show that the practical discrete adaptive modulation has the potential to achieve the rate very close to the capacity. The simulated AMC proves the well-designed AMC can achieve a rate close to the capacity.

In this paper, we have considered only the case with a single (peak power) constraint on input. As an extension, we can consider the cases in which both average power and peak power are simultaneously constrained [4], [5]. It is straightforward to study such complicated cases by rewriting the conditions, and similar results will be observed. This is because the CAD becomes discrete in many cases for many types of channels and constraints [7]. Similar comparisons between achievable rates and capacities under those conditions will provide useful guidelines for adaptive modulations. This could not be possible with the indirect approach in which the capacity is derived in terms of average power of input and constraints are discussed separately.

We have also restricted our discussion to the discrete-time input. To the best of our knowledge, there has been no direct comparison in the literature between the achievable rates with different constellations and the capacity under peak power constraint even in the case with a discrete-time AWGNC, the only exception being [9] and as we have demonstrated, the direct comparison for the discrete-time channel has yielded several novel quantitative observations regarding gaps between achievable rates with practical constellations and the capacity under peak power constraint. On the other hand, it has now been a common practice in the indirect approach to study the PAR in continuous-time domain, typically in terms of the complementary cumulative distribution function (CCDF) of PAR values. Another important direction of extending our analysis is therefore to consider peak power constraint on continuous-time input in the direct approach as well.

Acknowledgment

This work was supported by JSPS Grant-in-Aid No. 24560490 and 25120008.

References

[1] S. T. Chung and A. J. Goldsmith, "Degree of freedom in adaptive modulation: a unified view," *IEEE Trans. Commun.*, vol. 49, no. 9, pp. 1561–1571, 2001.

[2] C. E. Shannon, "A mathematical theory of communication," *The Bell System Tech. Journal*, vol. 27, pp. 379–423 and 623–656, 1948.

[3] F. H. Raab, P. Asbeck, S. Cripps, P. B. Kenington, Z. B. Popović, N. Pothecary, J. F. Sevic, and N. O. Sokal, "Power amplifiers and transmitters for RF and microwave," *IEEE Trans. Microw. Theory Tech.*, vol. 50, no. 3, pp. 814–826, 2002.

[4] J. G. Smith, "The information capacity of amplitude- and variance-constrained scalar Gaussian channels," *Inform. and Control*, vol. 18, pp. 203–219, 1971.

[5] S. Shamai (Shitz) and I. Bar-David, "The capacity of average and peak-power-limited quadrature Gaussian channels," *IEEE Trans. Inf. Theory*, vol. 41, no. 4, pp. 1060–1071, 1995.

[6] M. C. Gursoy, V. Poor, and S. Verdú, "The noncoherent Rician fading channel–part I: Structure of the capacity-achieving input," *IEEE Trans. Wireless Commun.*, vol. 4, no. 5, pp. 2193–2206, 2005.

[7] T. H. Chan, S. Hranilovic, and F. R. Kschischang, "Capacity-achieving probability measure for conditionally Gaussian channels with bounded inputs," *IEEE Trans. Inf. Theory*, vol. 51, no. 6, pp. 2073–2088, 2005.

[8] S. Ikeda and J. H. Manton, "Capacity of a single spiking neuron channel," *Neural Computation*, vol. 21, no. 6, pp. 1714–1748, 2009.

[9] R. R. Müller, U. Wachsmann, and J. B. Huber, "Multilevel coding for peak power limited complex Gaussian channels," in *Proc. of 1997 IEEE Int. Symp. on Inform. Theory*, June 1997, p. 103.

[10] *Digital Video Broadcasting (DVB); Second generation framing structure, channel coding and modulation systems for Broadcasting, Interactive Services, News Gathering and other broadband satellite applications (DVB-S2)*, ETSI, EN 302 307, V1.2.1, 2009.

[11] R. E. Blahut, *Modem Theory: An Introduction to Telecommunications*. Cambridge University Press, 2010.

[12] D. Tse and P. Viswanath, *Fundamentals of Wireless Communication*. Cambridge University Press, 2005.